Note: Electrostatic beams from a 5 T Penning–Malmberg trap

T. R. Weber, J. R. Danielson, and C. M. Surko
Department of Physics, University of California at San Diego, La Jolla, California 92093-0319, USA

(Received 16 August 2010; accepted 19 October 2010; published online 24 January 2011)

A procedure is described to extract beams from specially tailored electron plasmas in a Penning–Malmberg trap in a 4.8 T field. Transport to 1 mT is followed by extraction from the magnetic field and electrostatic focusing. Potential applications to positron beams are discussed. © *2011 American Institute of Physics*. [doi:10.1063/1.3514150]

With recent progress in antimatter research, there is an increasing need for high quality positron beams.[1–3] We described previously a high field Penning–Malmberg (PM) trap for the creation of high quality, magnetically guided beams.[4] It has been established that such a high field (HF) trap can be filled with positrons and the resulting plasmas can be manipulated in a manner similar to electrons.[5] Thus, the experiments described here, done with electron plasmas for increased data rate, are relevant to positron beams as well.

Using pulsed extraction from the PM trap, electron beams were created with small transverse spatial extent (i.e., Gaussian radial profiles with radii to 1/e $\rho_b \leq 50$ μm), low rms energy spreads $\Delta E \leq 30$ meV, and high reproducibility ($\Delta N_b/N_b < 5\%$, where N_b is the total number of beam particles).[6–8] However, those beams reside in a large magnetic field and are not useful in applications requiring a beam in a field-free region.[1,9] Such applications include angularly resolved scattering from atomic and molecular targets;[9,10] a positron reaction microscope;[11] exploiting "remoderation" techniques to enhance beam brightness;[12,13] and the formation of Ps_2 and a Ps-BEC.[3]

Described here is a technique to create electrostatic beams originating from plasmas in a 4.8 T magnetic field. Formation of the initial beam is described in Ref. 7. Beam extraction from the field is then done in two stages: the beam is first transported adiabatically to 1 mT, followed by a fast (i.e., non-adiabatic) extraction to zero field. Once in this zero-field region, the beam is focused using an Einzel lens to demonstrate electrostatic beam control and the capability to reduce the transverse beam size.

The experimental apparatus is illustrated in Fig. 1. The slow extraction is accomplished by allowing the field to fall off naturally as the particles exit the HF magnet. Then opposing coils (at $z \approx 150$ and 175 cm in Fig. 1) shorten the length of the experiment and define more precisely the spatial location of the transition to zero field. A magnetic shield made of sheets of Permalloy (relative magnetic permeability $\mu_r \sim 2 \times 10^4$), with a centered front-cap hole of diameter $d=5.08$ cm, creates the zero field region. This hole forms a tight fit around the necked-down portion of the beam tube ($z \approx 175$ cm in Fig. 1). The fast extraction occurs at the front-cap hole ($z \approx 180$ cm in Fig. 1) where $B = 1 \rightarrow 0$ mT over a distance $\delta z \approx 5$ cm. The currents required in the two opposing coils were first estimated by numerical calculation then determined more precisely experimentally.

In the fast extraction from the field, the particles make the transition to $B=0$ sufficiently quickly that, although the Lorentz force from the flaring magnetic field changes their velocity, they have no time to move radially.[14] As a result, the radial positions of the particles remain constant while they undergo an increase in the azimuthal component of their velocity.

Once inside the Permalloy shield, the beam is guided only by electrostatic fields (i.e., a so-called electrostatic beam). As illustrated in Fig. 1, it is then focused with an Einzel lens and the beam properties measured using an apertured collector cup mounted on a movable linear feedthrough. The lens consists of three identical hollow cylinders (5.7 cm in length and inner diameter). The lens is operated in an acceleration-deceleration mode with the center electrode biased to a large positive voltage V_L and the two exterior electrodes grounded.

The beam is aligned by first imaging it on a phosphor screen temporarily mounted near the beginning of the Permalloy shield. The (adjustable) orientation of the HF magnet is aligned until the beam is visible on the screen. Then saddle coils, placed at the beginning of the first opposing solenoid ($z \approx 140$ cm in Fig. 1), are used to center the beam in the tube.

The phosphor screen is then removed and the central beam intensity is monitored using the collector cup with a centered hole of diameter $d=0.24$ cm. The focal position is found by moving the collector in the z direction to maximize the collector signal. The saddle coils are then readjusted to center the beam more precisely, and this process iterated as necessary. It must be repeated every few days to account for small changes in the experiment. The total beam-pulse intensity is measured upstream on a collector plate. This measurement and the collector-cup signal are used to calculate the absolute fraction of the beam that passes through the collector-cup aperture.

A measure of the (non)adiabaticity of the beam transport process is $\gamma = \tau_{cyc}(1/B)dB/dt$, where τ_{cyc} is the electron gyro-period and dB/dt is the rate of change of the magnetic field in the beam frame. When $\gamma \ll 1$, the beam particles conserve the adiabatic invariant $J = E_\perp/B$, where $E_\perp$ is the kinetic energy in the motion perpendicular to the magnetic field.[15] Qualitatively, the particles remain on their respective magnetic field lines while undergoing small-scale gyro-motion. For the experiments described here, over most

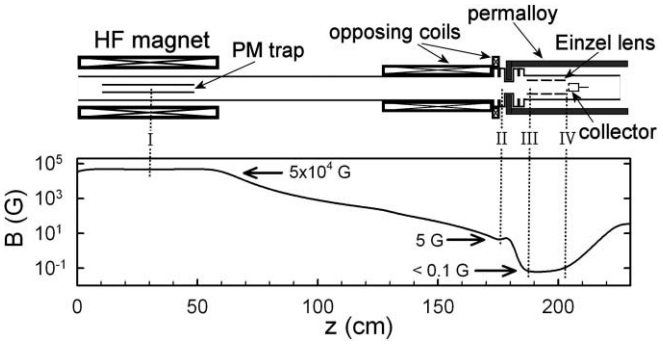

FIG. 1. (above) Schematic diagram of the experiment illustrating the magnetic extraction, followed by the Einzel lens spatial focus to a collector cup. (below) The on-axis magnetic field oriented in the z direction, $B_z(r=0)$. Saddle coils used to align the field at $z\approx140$ cm are not shown.

of the slow reduction in B, $|\gamma|<0.01$, while in the last 10 cm, $|\gamma|$ rises to 0.6.

Beam pulses (≈5 μs in duration) were extracted from a parent plasma with parameters: total number of particles $N\approx3.5\times10^8$ electrons; density $n\approx1.2\times10^{10}$ cm^{-3}; temperature $T\approx0.1$ eV; radius $R_p\approx230$ μm; and length $L_p\approx15$ cm. The beam has a Gaussian radial profile, with a 1/e radius $\rho_b=65$ μm in the 4.8 T field. The number of particles per pulse is $N_b\approx3.4\times10^6$. The beam transport energy is ≈30 eV, as set by the confining electrode potential and the plasma potential. The perpendicular energy spread is Maxwellian with $T=0.1$ eV, while the parallel energy spread is non-Maxwellian.[8] The rms spread in the total energy is $\Delta E\approx0.24$ eV.[8] The relevant beam parameter is $\xi=eN_b/L_pT=0.4$, and the relevant plasma parameter is $R_W/\lambda_D=500$, where $2R_W$ is the inner diameter of the electrodes and λ_D is the Debye length of the parent plasma.[8] These parameters have been shown to precisely define the beam width ρ_b and rms energy spread ΔE.[8] The beam particles remain on field lines up to the point of fast extraction resulting in a beam radius at that point of 0.45 cm.

Shown in Fig. 2 is the percentage of beam particles transmitted through the collector aperture as a function of aperture position z for $V_L=5$ kV, where $z=0$ now corresponds to the end of the lens ($z\approx205$ cm in Fig. 1), and the sign convention for z is that used in Fig. 1. The focus occurs at $z\approx5$ mm, where $\approx43\%$ of the beam passes through the aperture. Note the marked asymmetry of the focusing curve as a function of z, showing a fast rise followed by a slower decline beyond the focus.

The lens voltage was varied, and curves similar to Fig. 2 were measured. The percentage of beam particles passing through the aperture at the lens focus as a function of V_L is plotted in Fig. 3.[16] The transmission coefficient increases as a function of V_L and then begins to saturate. For the maximum at $V_L=6$ kV, $\approx52\%$ of the beam passes through the aperture. Also plotted in Fig. 3 is the focusing position of the lens as a function of V_L. As expected, increasing the lens voltage results in a more tightly focused beam with a focal position closer to the lens.

Complementary numerical simulations to model the fast extraction and electrostatic focusing will be reported

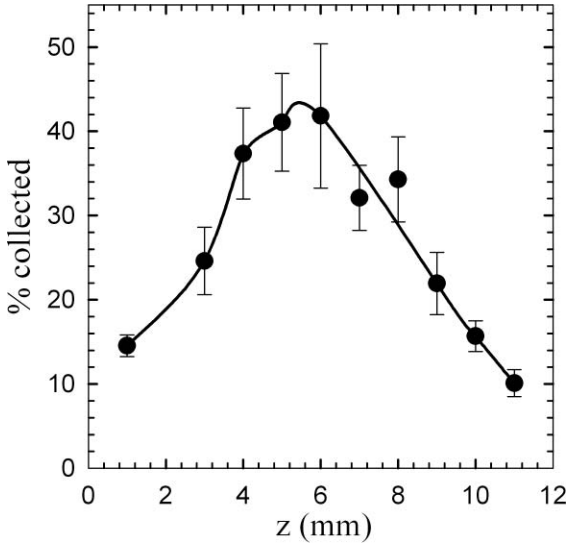

FIG. 2. The percentage of the beam transmitted through the collector aperture ($d=0.24$ cm) versus the z-position of the aperture (•). Here, $V_L=5$ kV, $z=0$ corresponds to the exit end of the lens, and the initial beam parameters are $\xi=0.4$, $\rho_b=65$ μm and $\Delta E=0.24$ eV. The solid line is a spline fit and guide to the eye.

elsewhere.[17] The results agree well with the curves plotted in Figs. 2 and 3. They indicate that significant lens aberrations are present at higher values of V_L (e.g., $V_L>4$ kV). These aberrations appear to be responsible for the asymmetry seen in Fig. 2, and the saturation shown in Fig. 3.

In related work, theoretical expressions have been developed for the moments of the beam energy distribution, valid in the limit $\xi<0.5$.[17] These expressions can be used to predict the beam emittance, which is a key measure of beam quality.[18] Assuming a Gaussian radial profile with 1/e radius ρ_b, and extraction from a plasma at temperature T in the 4.8 T field, the generalized invariant emittance is found to be,[17,19]

$$\epsilon^* = \rho_b\sqrt{T_\perp}\left[1+\left(\frac{\rho_b}{2\rho_c}\right)^2\right]^{1/2}, \tag{1}$$

where ρ_c is the cyclotron radius in the local magnetic field and $T_\perp=T(B/B_i)$, with B_i the field at the point of beam formation in the HF trap. Here, $T_\perp$ is the local value of

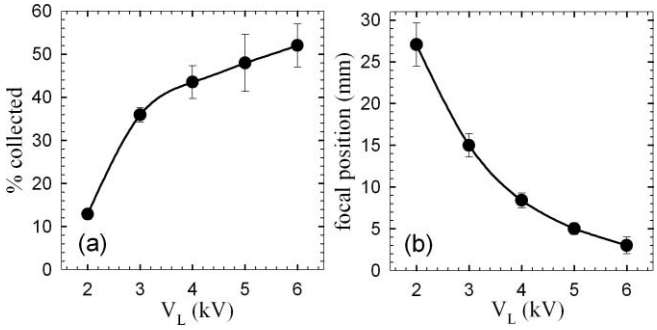

FIG. 3. (a) The percentage of the beam particles transmitted through the aperture versus V_L (•) for an initial beam of $\rho_b=65$ μm in the HF. (b) The focusing position of the lens plotted for each value of V_L (•). Solid lines in both (a) and (b) are spline fit curves to guide the eye.

the particle energy in the motion perpendicular to B. The second term Eq. (1), $(\rho_b/2\rho_c)^2$, typically dominates for the magnetically guided beams described here, as $\rho_c \ll \rho_b$. The parameter ϵ^* has the same numerical value in and out of the field and reduces to the conventional invariant emittance $\epsilon = \rho_b \overline{E}_\perp^{1/2}$ out of the field. It is exact for Gaussian beams extracted from plasmas at temperature T in the limit of small ξ.[17] Fixed at the point of beam formation in the 4.8 T magnetic field, $\epsilon^* = 0.3$ cm-$(\text{eV})^{1/2}$ for the beam described here.

Previously, we demonstrated that one can use the tools available in UHV HF Penning–Malmberg traps, namely rotating wall radial plasma compression and cyclotron cooling, to improve beam quality. This note reports a further advancement to extract beams from the confining magnetic field to create a class of electrostatic beams. Experimentally, beam alignment can be maintained while reducing B by a factor of 5×10^3 before fast extraction, thereby minimizing the otherwise unavoidably large increases in perpendicular energy. The beam is then focused using an Einzel lens to demonstrate electrostatic beam control. Use of a more sophisticated extraction method, employing a grid or radial spoke arrangement made of high-permeability material, could create even higher quality beams by decreasing further the effects from the flaring magnetic field.[20]

For the intended positron applications, the beam emittance achieved here is only roughly comparable to current cutting-edge positron beam systems. For example, using positrons beams obtained directly from a buffer gas positron accumulators, values of $\epsilon^* \approx 0.12$ cm-$(\text{eV})^{1/2}$ have been achieved in a 50 mT field.[21] However, these types of systems do not have the UHV-quality vacuum or the high storage capabilities of the HF trap used here. Further, in the approach described here, the transverse beam width, and hence the beam emittance, is set by the parent-plasma Debye length $\lambda_D \propto \sqrt{T/n}$. Thus, colder plasmas obtained by cooling the trapping electrodes (and hence enhancing the cyclotron cooling) and possible improvements in plasma compression techniques could be used to produce higher quality positron beams with $\epsilon^* < 0.05$. Moreover, these beams would be very cold (e.g., $\Delta E < 7$ meV) because, for small ξ, the extracted electrostatic beam maintains the initial energy spread of the parent plasma. Thus, this technique has the potential to produce a class of cold positron beams that are relatively ideal for spectroscopy experiments.

We wish to acknowledge the expert technical assistance of E. A. Jerzewski. This work was supported by the NSF Grant No. PHY 07-13958 and the DoE Grant No. DE-SC0004661.

[1] A. P. Mills, Jr., Appl. Phys. **22**, 273 (1980).
[2] A. David, G. Kogel, P. Sperr, and W. Triftshäuser, Phys. Rev. Lett. **87**, 067402 (2001).
[3] A. P. Mills, Jr., D. B. Cassidy, and R. G. Greaves, Mater Sci. Forum **445–446**, 424 (2004).
[4] J. R. Danielson, P. Schmidt, J. P. Sullivan, and C. M. Surko, in *Non-Neutral Plasma Physics V*, edited by M. Schauer, T. Mitchell, and R. Nebel (American Institute of Physics, Melville, NY, 2003), p. 149.
[5] L. V. Jørgensen, M. Amoretti, G. Bonomi, P. D. Bowe, C. Canali, C. Carraro, C. L. Cesar, M. Charlton, M. Doser, A. Fontana, M. C. Fujiwara, R. Funakoshi, P. Genova, J. S. Hangst, R. S. Hayano, A. Kellerbauer, V. Lagomarsino, R. Landua, E. Lodi Rizzini, M. Macrí, N. Madsen, D. Mitchard, P. Montagna, A. Rotondi, G. Testera, A. Variola, L. Venturelli, D. P. van der Werf, and Y. Yamazaki (ATHENA Collaboration), Phys. Rev. Lett. **95**, 025002 (2005).
[6] J. R. Danielson, T. R. Weber, and C. M. Surko, Appl. Phys. Lett. **90**, 081503 (2007).
[7] T. R. Weber, J. R. Danielson, and C. M. Surko, Phys. Plasmas **15**, 012106 (2008).
[8] T. R. Weber, J. R. Danielson, and C. M. Surko, Phys. Plasmas **16**, 057105 (2009).
[9] C. M. Surko, G. F. Gribakin, and S. J. Buckman, J. Phys. B **38**, R57 (2005).
[10] W. E. Kauppila and T. S. Stein, Adv. At., Mol., Opt. Phys., **26**, 1 (1990).
[11] J. Ullrich, R. Moshammer, A. Dorn, R. Dorner, L. Ph. H. Schmidt, and H. Schmidt-Bocking, Rep. Prog. Phys. **66**, 1463 (2003).
[12] A. P. Mills, Jr., Appl. Phys. **23**, 189 (1980).
[13] R. G. Greaves and C. M. Surko, Nucl. Instrum. Methods Phys. Res. B **192**, 90 (2002).
[14] N. Oshima, R. Suzuki, T. Ohdaira, A. Kinomura, T. Narumi, A. Uedono, and M. Fujinami, J. Appl. Phys. **103**, 094916 (2008).
[15] J. A. Young and C. M. Surko, Nucl. Instrum. Methods Phys. Res. B **247**, 147 (2006).
[16] The data point at the focal point in Fig. 2 differs slightly from that at $V_L = 5$ kV in Fig. 3, likely due to run-to-run differences in the experimental conditions.
[17] T. R. Weber, J. R. Danielson, and C. M. Surko, "Electrostatic beams from tailored plasmas in a Penning-Malmberg trap," Phys. Plasmas (in press).
[18] M. Reiser, *Theory and Design of Charged Particle Beams* (Wiley, New York, 1994).
[19] While approximate expressions for ϵ^* have been presented previously, we do not find this expression in the literature.
[20] D. Gerola, W. B. Waeber, M. Shi, and S. J. Wang, Rev. Sci. Instrum. **66**, 3819 (1995).
[21] D. B. Cassidy, S. H. M. Deng, R. G. Greaves, and A. P. Mills, Rev. Sci. Instrum. **77**, 073106 (2006).